Journal of Engineering and Applied Sciences 11 (Special Issue 2): 3167-3176, 2016
ISSN: 1816-949X

Finite Element Study of Reinforced Concrete Deep Beams with Rectangular Web Openings

Iman Bahrami Chegeni and Ahmad Dalvand
Faculty of Engineering, Lorestan University, Khorramabad, Iran

Abstract: The shear behavior of reinforced concrete deep beams is one of the most influential factors on the total behavior of the structure. The arrangement of stirrups in concrete members, especially in beams has a considerable effect on ductility and hysteresis behavior of the structure. The shear behavior plays a great role in gravity loads of the structure and its failure mechanism. Due to their different behavior in compare to flexural members, studying the cracking pattern in concrete deep beams seems necessary. In this study the cracking pattern of concrete deep beams with web openings is considered. To do this, finite element models of six concrete deep beams with web openings and without shear reinforcement were built by ANSYS Software and verified using experimental results. The modeled beams had the same properties, except for the size and place of the opening. The analysis results showed that both shear capacity and stiffness reduced by the increase in the opening area. Collapse of the concrete beam was due to expansion of cracks on corners of the opening, parallel to compression member of truss.

Key words: Reinforced concrete deep beam, shear behavior, opening, finite element, crack pattern, failure mechanism

INTRODUCTION

Ductility is one of the most important factors in designing of especial structures such as bridges and high-rising buildings. Beams of these structures are categorized as deep beams, therefore studying the failure mechanism of main beams and the effect of their behavior on total behavior of these structures is highly important (Leong and Tan, 2003; Gunel and Ilgin, 2007). In older studies, the design of deep beams was done similar to normal flexural beams but after more studies it was cleared that their behavior is different than normal flexural beams. Using concrete deep beams in high-rising buildings particularly in tubular system as linking beams and also in bridging is very common. In recent years, many studies have been carried out to investigate the behavior of concrete deep beams. In 2006, shear resistance of concrete deep beams with steel profile in the web was evaluated by Lu (2006). In that study a model for predicting the behavior of these beams and also their failure and rupture modes was presented that correlated with experimental results properly. In 2005, the effect of using external FRP fiber on the shear behavior of concrete deep beams was studied by Islam *et al.* (2005).

Based on results of their study it was concluded that angled pattern FRP has better effect in performance of concrete deep beams. The study of Zhang and Tan (2007) and Islam *et al.* (2005) resulted in presenting a modified model of Strut and Tie method to evaluate shear resistance of both simple and continuous concrete deep beams. Very few studies has been conducted to examine crack pattern in concrete deep beams with openings. A deep concrete beam prototype was built in laboratoryto investigate crack pattern in deep concrete beam with opening. The 6 concrete deep beams with web openings and without shear reinforcement were modeledusing ANSYS Software's finite element and verified by experimental model. The modeled beams had same properties with differences in dimensions and positions of openings.

MATERIALS AND METHODS

For the experimental model, a 1500 mm long, 250 mm high and 200 mm wide deep concrete beam was built with a 1000 mm net span. To provide proper development length for bending reinforcement, both ends of the beam were continued for 250 mm. reinforcing details and dimensions and support conditions are respectively shown in (Fig. 1 and 2).

A concentrated load was applied to the middle of the experimental model with simple support conditions. Loading was done statically and at 5 kN increments. The

Corresponding Author: Iman Bahrami Chegeni, Faculaty of Engineering of Lorestan University, Khorramabad, Iran

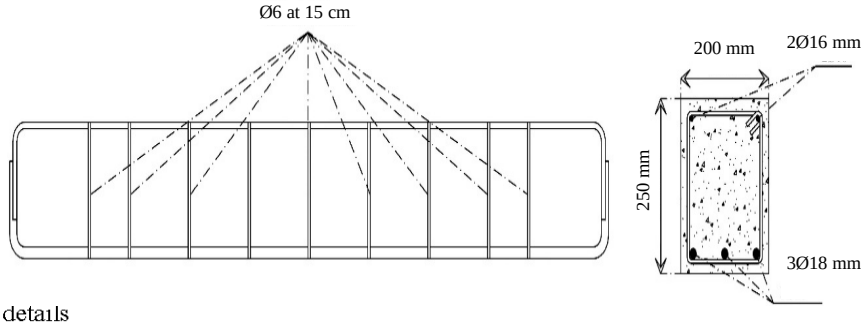

Fig. 1: Reinforcement details

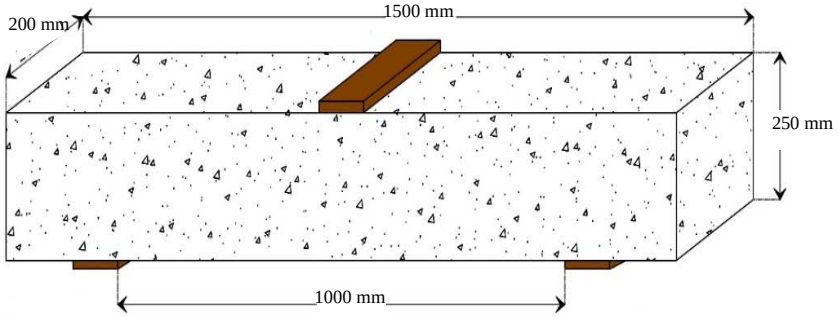

Fig. 2: Beam dimensions and support condition (Damian *et al*., 2001)

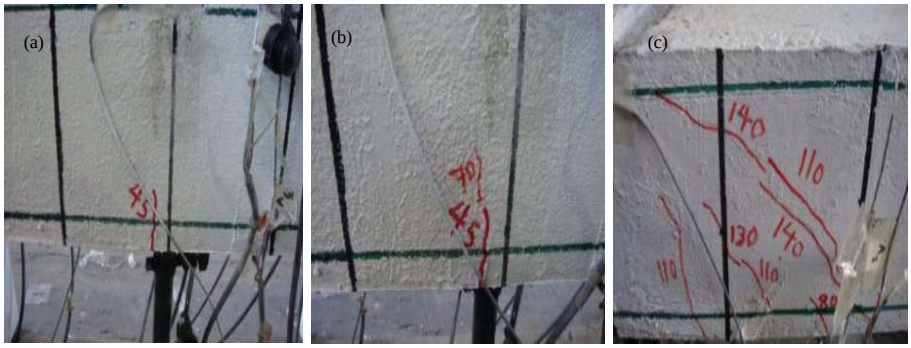

Fig. 3: a) First crack appearance; b) Flexural crack development; c) Shear crack development

first crack was developed at 45 kN loading and 0.65 mm displacement as aflexural crack at the beam's mid-span and the maximum moment location as depicted in (Fig. 3). By increasing the loading to 70 kN next cracks also appeared under concentrated load position as flexural cracks. This is shown on (Fig. 3). By rising the loading to 110 kN the first shear crack was formed on the beam as shown in (Fig. 3).

The number of flexural cracks also increased by this point. By 155 kN of loading the length and width of shear cracks increased and rupture path emerged. At 178 kN the beam collapsed due to shear failure. The shear cracks initiated from supports and ended at loading point, this is shown in (Fig. 4). Afterward, due to rupture and plunge in loading capacity of the beam and surge in displacements at the middle of the beam, the experiment was halted. The load-displacement diagram of the experimental beam is shown in (Fig. 5). The final deflection was 5.05 mm considering the 10-15% reduction of the final load. Because of beam's shear failure no yielding was observed in longitudinal bars. Up to the failure point the beam performed as a shear beam and shear cracks gradually initiated from supports and reached out to the loading point. Position of the main crack is illustrated in Fig. 4. The alignment angle from the longitudinal axis of the beam is around 35°C.

Finite element model verification: Concrete has a complicated failure mechanism because of complicated nonlinear behavior and its cracking in tension and

Fig. 4: Failure surface of unreinforced concrete under triaxial condition

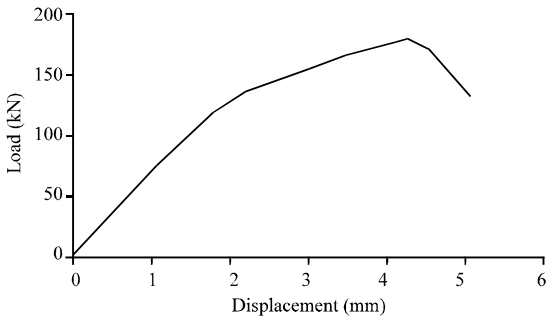

Fig. 5: load-displacement of experimental beam

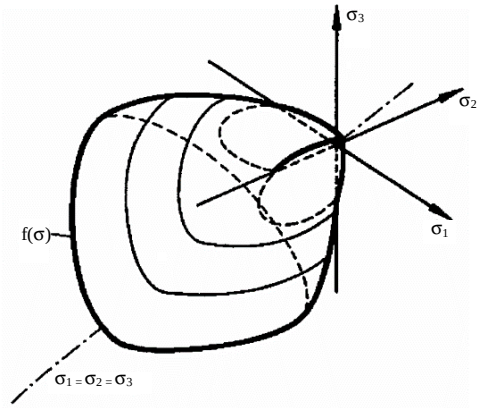

Fig. 6: Shear failure of concrete beam

crashing in compression character. Various failure criteria has been introduced up to now. William-Warnke model is one of the most reputable and comprehensive criteria for concrete failure. In order to present an analytical model that is close to reality any failure criteria chosen for analysis should consider effects of cracking, crushing and aggregate interlock. Willam and Warnke presented a model for triaxial failure surface of unconsolidated unreinforced concrete. This mathematical model is a sextant of the principal stress space provided that order is current. These are the main stress components. The failure surface in principal stress space is depicted in (Fig. 6).

In this study, Eq. 1-3 are used to form uniaxial compression stress-strain curve of the concrete:

$$f = \frac{E_c \varepsilon}{1 + \left(\frac{\varepsilon}{\varepsilon_0}\right)^2} \quad (1)$$

$$\varepsilon_0 = \frac{2f_c'}{E_c} \quad (2)$$

$$E_c = \frac{f}{\varepsilon} \quad (3)$$

Where:

f = Tension (Mpa)

f_c = Strain is strain at ultimate compression strength and is compression

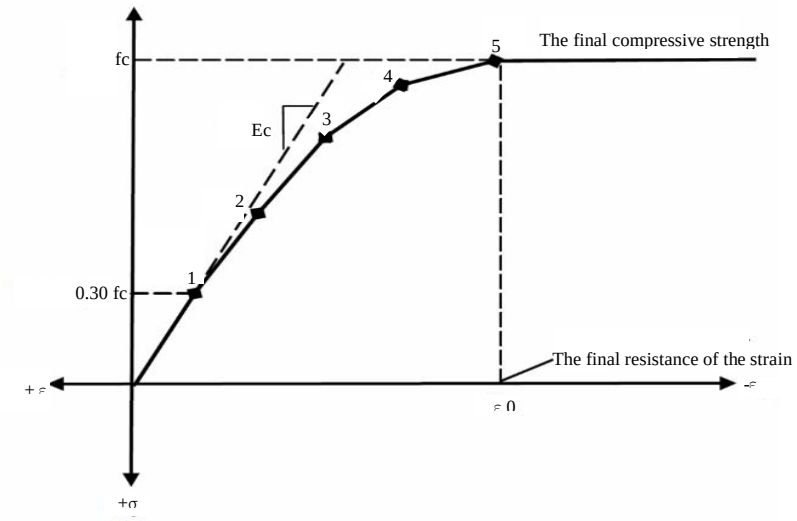

Fig. 7: Simplified stress-strain curve

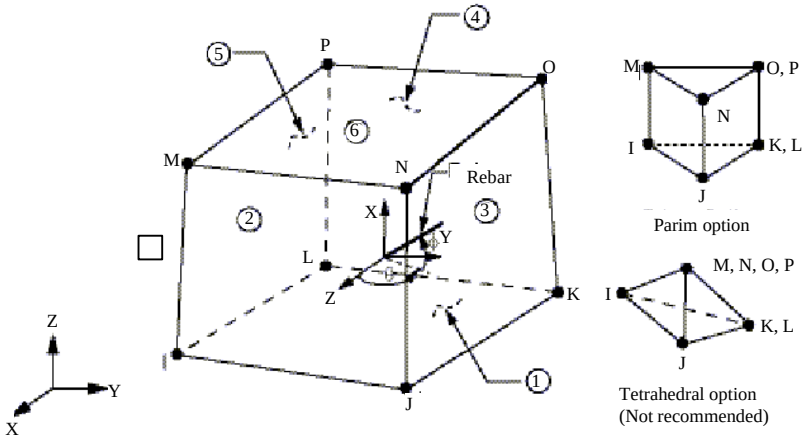

Fig. 8: Solid 65 element geometry figure

strength of cylindrical specimen. The simplified stress strain relation that is used in this study is shown in (Fig. 7). The strain-stress diagram consists of 6 points connected to each other by straight lines. It starts from zero strain and stress point. Point 1 at is used for linear stress-strain zone (Eq. 3). Numbers 2, 3 and 4 are derived from equation 1 in which is calculated by equation 2. Point 5 is located at (ε_o, f_c). It is also assumed that the behavior after point 5 is complete plastic. To validate the results of the software and compare it to experimental results, the examined beam was modeled by ANSYS as well. The Solid 65 element was used to model concrete. This element is capable to model 3D concrete (reinforced and unreinforced). This element is able to model crashing at compression and cracking at tension. This 8 node element has three transitive degrees of freedom at each node at X, Y and Z directions. The geometry of the Solid65 element is illustrated at (Fig. 8). Link 8 element was used to model reinforcing bars which is an element with three transitive degree of freedom at each end but has no bending resistance and is appropriate to model bars. Element solid 45 was used to model support plates and loading plates.

Using experimental model's specifications, the finite element model of concrete beam was built in ANSYS as shown in (Fig. 8 and 9). Concrete strength during experiment was taken 35 Mpa. And Table 1-reference source not found-results of tensile test on stirrups and rebars. preparing load-displacement curve for numerical model that agrees with load-displacement curve of experimental specimen is time consuming. The final load displacement curve of analytical beam is as shown on Fig. 6. Experimental and analytical model match relatively well. Based on this (Fig. 10), the error of the ultimate load and ultimate displacement of the analytical model compared to experimental model is 4 and 7%, respectively.

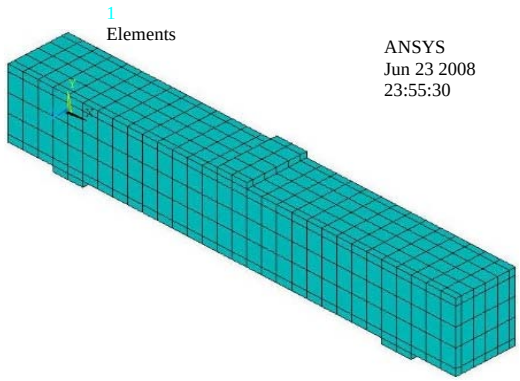

Fig. 9: FEM Model of the experimental model

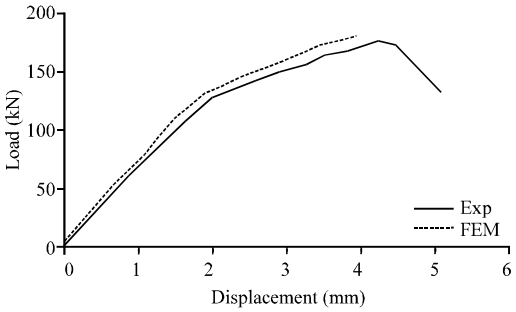

Fig. 10: truss mechanism

Table 1: Results of tensile test on strrups and rebars

Bar No.	Diameter (mm)	Yielding tension (Mpa)	Ultimate tension (MPa)
1	6	255	290
2	10	330	360
3	18	480	510

Table 2: Corresponding displacement and loading to cracking, yielding and ultimate states of the calibration beam's nonlinear analysis

	Cracking		Emerging deep shear crack		Ultimate amounts	
Specimen	P_{cr} (kN)	Δ_{cr} (kN)	P (kN)	Δ (mm)	P_u (kN)	Δ_u(mm)
Experimental specimen	45	65/0	110	64/1	175	26/4
Analytical specimen	50	67/0	110	53/1	5/181	2/4

Cracking load of finite element has 5% difference in compare to experimental model. This finite element model could be applied to other finite element models as well. Both displacements and loadings of ultimate and cracking stages are shown in Table 2.

Determining shear resistance in deep beams: Deep beams are members that transfer most of the loads to the supports by forming inner continuous truss. In recent years, some methods to design deep beams has been presented to design deep beams including strut and tie model. Due to its good compression resistance and buckling resistance at compression, concrete is assumed to be strut and due to good tension resistance of bars they are assumed to be ties of the truss. As shown in Fig. 10, α is cracking angle and β is shear bar's angle to horizon. According to Fig. 10, relation between shear and bars tension is expressed as Eq. 4-6:

$$S = jd(\cot\alpha + \cot\beta) \tag{4}$$

$$V_s = C_d \sin(\alpha) = T_s \sin(\beta) \tag{5}$$

$$V_s = C_d \sin(\alpha) = T_s \sin(\beta) \tag{6}$$

According to ACI (2002), deep beams are those kind of members that the load is applied on one surface and the supports are on the opposite surface so the compression truss can form between supports and loading point (Tan *et al*., 2003) . According to ACI (2002), a deep concrete beam's length should be <4 times of its height or the distance of loading point from the support should be less than two times of the beam's total height. Openings in deep beams are located to ease the placing of air conditioner channels, electrical facilities and computer network wiring. The shear behavior of such beams complicates and their loading capacity decreases if the load transmission path is changed by these openings. Based on the study by Kong and Sharp (1977) shear resistance of deep beams without openings and reinforcement is defined by Eq. 7:

$$\frac{T_s}{S} = \frac{V_s}{S\sin\beta} = \frac{V_s}{S\sin\alpha} = \frac{V_s}{jd(\cot\alpha + \cot\beta)\sin\beta} \tag{7}$$

Which is concretes tension stress and is a coefficient that is equal to 1.4 for normal concrete and for lightweight concrete is 1.35. Coefficientis equal to 300 Mpa for deformed (ribbed) bars and for plain (simple) bars is = 130 Mpa y is depth of longitudinal bars, x is net shear span is beam's width, h is total height of the section, final area of steel bars and is the angle as shown in Fig. 11. In relation 7, V_n is shear resistance of deep beam with no openings. If the opening crosses the path between loading point and support points, then Eq. 8 should be used instead of Eq. 7. In this equation, coefficients and in relation 8 are shown in Fig. 8.

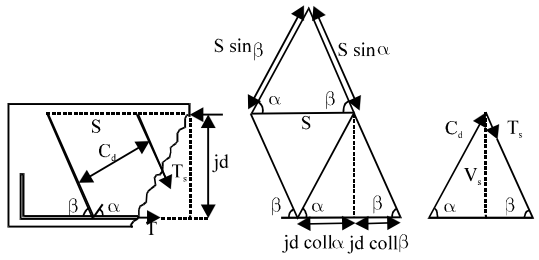

Fig. 11: Effective parameters in concrete deep beam beahvior

$$V_n = C_1\left[1-0.35\frac{X}{h}\right] f_t' b_w h + C_2 A_s \frac{y}{h} \sin^2\theta_3 \quad (8)$$

Based on Mohr-Colomb modified model, Tan *et al.* (1997) has introduced a new model. In this model, the ultimate shear resistance with no openings and shear reinforcement is calculated as Eq. 9 by starting with main stress on the bottom of the nodal area. In Eq. 9 A_c is transverse cross section area of compression truss as shown in Eq. 10. Besides A_c is cross section area of the concrete beam.

$$V_n = \frac{1}{\frac{\sin 2\theta}{f_t A_c} + \frac{1}{f_c' A_{str} \sin\theta}} \quad (9)$$

$$A_{str} = b_w \left(w_t \cos\theta + l_p \sin\theta\right) \quad (10)$$

Equation 10, w_t is the depth of lower nodal area and I_p is the width of support plates. In relation 9, f_t is the share of total resistance of concrete and steel bars that is expressed as relation 11 in which is total area of longitudinal bars and is their yielding stress.

$$f_t = \frac{2 A_s f_y \sin\theta}{A_c/\sin\theta} + f_t' \quad (11)$$

Equation 11, f_t is tension resistance of concrete. In case of opening in the beam, the ultimate shear resistance of beam is calculated by Eq. 12:

$$V_n = \frac{1}{\frac{\sin 2\theta_3}{f_{t3} A_{c3}} + \frac{1}{f_c' A_{str3} \sin\theta_3}} \quad (12)$$

$A_{c3}$and are calculated by Eq. 13-15:

$$A_{c3} = b_w k_2 h \quad (13)$$

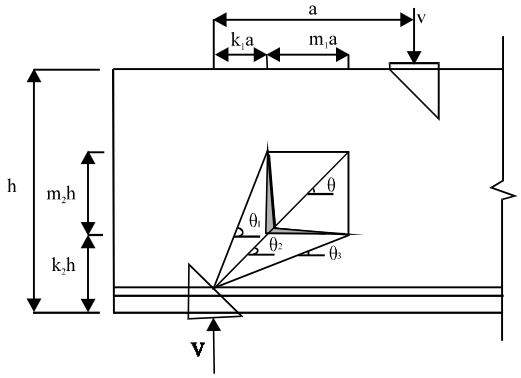

Fig. 12: opening position parameters

Table 3: Dimension and specifications of models and openings

Specimen no.	Z 1 (mm)	Z (mm)	Z_3 (mm)	Z_4 (mm)	θ_3 (degree)	h×b $(mm)_2$
B1	200	150	175	300	30	200×500
B2	200	100	200	300	34	200×500
B3	150	150	175	325	32	200×500
B4	150	100	200	325	36	200×500
B5	100	150	175	350	35	200×500
B6	100	100	200	350	39	200×500

$$f_{t3} = \frac{2 A_s f_y \sin\theta_3}{A_{c3}/\sin\theta_3} + f_t' \quad (14)$$

$$A_{str3} = b_w \left(w_t \cos\theta_3 + l_p \sin\theta_3\right) \quad (15)$$

Effects of openings: In this study to investigate the effect of opening on the behavior of concrete deep beams, 6 finite element beam with web openings models were built in ANSY as shown in (Fig. 12). Dimension and specifications of models and openings are represented in Table 3.

The net shear span width for all specimen is 350 mm. h parameter, shown in (Table 3) is the total height of concrete beam's cross section. The height and width for all beams is 500 and 200 mm, respectively. Openings are located symmetrically on both sides of loading point. Center of all openings is on the line connecting loading point to each support. Net shear span to total height ratio is 0.7 for all specimen. In all specimen the width of openings is a percantage of net shear span. Opening height is also a percent of total height of the cross section. All modeled beams have 1472 mm^2 of longitudinal bars and 402 mm^2 of compression bars. There is no shear bars considered in the modeling. It also should be mentioned that opening widths are considered = 0.28, 0.43 and 0.57 of net shear span. Besides, opening height is chosen to be 0.2 and 0.3 of total cross section height. All beams have the same longitudinal bars and no shear stirrups. All finite element beams were imposed to concentrated loading at mid-span

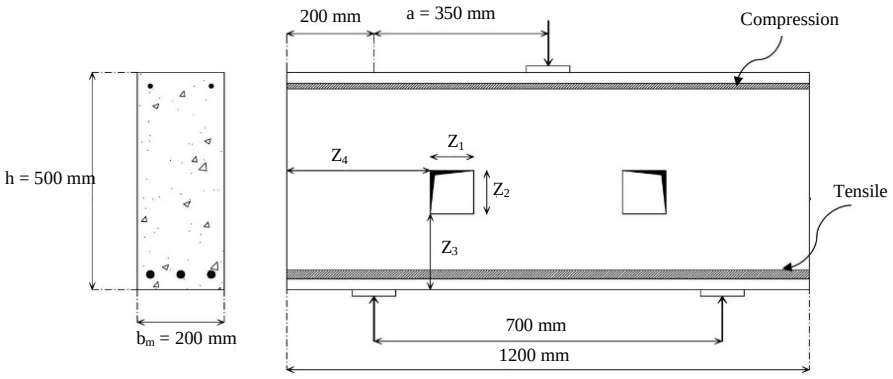

Fig. 13: FEM models: a) B1; b) B2; c) B3; d) B4; e) B5 and f) B6

up to failure point. Compression resistance of sample concrete in modeled beams is taken to be 35 MPa. Longitudinal bars of finite element models and experimental models are the same. Modeled beams in ANSYS are represented in (Fig. 13).

RESULTS AND DISCUSSION

Evaluating beams with opening's behavior: Load capacity and cracking pattern of specimen were compared after their analysis were done. Furthermore results of finite element specimen were compared to results from theoretical relations.

loading capacity: Force-displacement diagram of mid-span is shown in Fig. 11 for 6 beams. As shown in (Fig. 14), B6 specimen has the most load capacity, 183.3 and specimen B1 has the least load capacity = 80.9 kN. The maximum load capacity is 2.27 times of the least load capacity. Analyzed models are split in 3 groups. First group includes B1 and B2 Models, second group includes B3 and B4 Models and third group includes B5 and B6. They are grouped based on opening height. The opening position in each group is the same from each end of the beam. Displacement and cracking load of specimens is listed in Table 4.

As shown in Table 4 by decreasing opening width in each group, cracking load and ultimate load increases which causes an increase in cracking displacement and ultimate displacement. The increase in cracking displacement and ultimate displacement of second specimen compared to first specimen for first, second and third groups is 19 and 30, 5 and 19%, 18 and 7%, respectively. The ultimate load and ultimate displacement increased 28 and 8%, 19 and 6%, 4 and 11%, respectively for first, second and third groups. Based on these results, by decreasing the size of openings the maximum load and the area under force-displacement curve increases.

Table 4: Results of finite element analysis

Beam No.	Δ_{cr} (kN)	P_{cr} (kN)	Δ_u (mm)	P_u (kN)	Area under FEM curve kN (mm)	Percent of opening area to side area of beam
B1	32/0	1/17	91/2	9/80	116	10
B2	382/0	2/22	15/3	6/103	163	7/6
B3	56/0	56/31	96/3	3/134	253	5/7
B4	59/0	4/37	19/4	6/159	321	5
B5	79/0	3/43	22/5	3/176	447	5
B6	93/0	4/46	81/5	3/183	522	33/3

Table 5: Comparison between results of finite element analysis and theoretical relations

Beam no.	FEM Model P_{u_FEM} (kN)	Theoretical model Δ_{u_TH} (kN)	Difference % Pu FEN P_{u_Th}/P_{u_FEM}
B1	9/80	1/74	33/8
B2	6/103	8/96	52/6
B3	3/134	7/120	1/10
B4	6/159	2/147	78/7
B5	3/176	6/154	31/12
B6	3/183	3/163	26/9

The changes in area under force-displacement curve of mid-span for different angles is illustrated in Fig. 12. This curve consists of three zones that each one corresponds to one group. Based on this figure at each group the area under load-displacement curve increases by the increase in. In the first group, the area under force-displacement curve surges by 41% as increase 13% which indicates the sensitivity of this parameter to angle variations.

For second and third groups, the increase of area under load-displacement curve is respectively 27% and 17% for 12.5 and 11% of increase in. Furthermore in each group and area under force-displacement curve increased by decreasing the height of the opening while keeping the width unchanged.alters between 30 and 39°. In other words it has a 30% growth rate while the area under force-displacement curve for the first group has a 350% growth rate compared to the third group.Figure 15 and 16 shows the change curve of concentrated load against Z_2/L_1 parameter (Table 5).

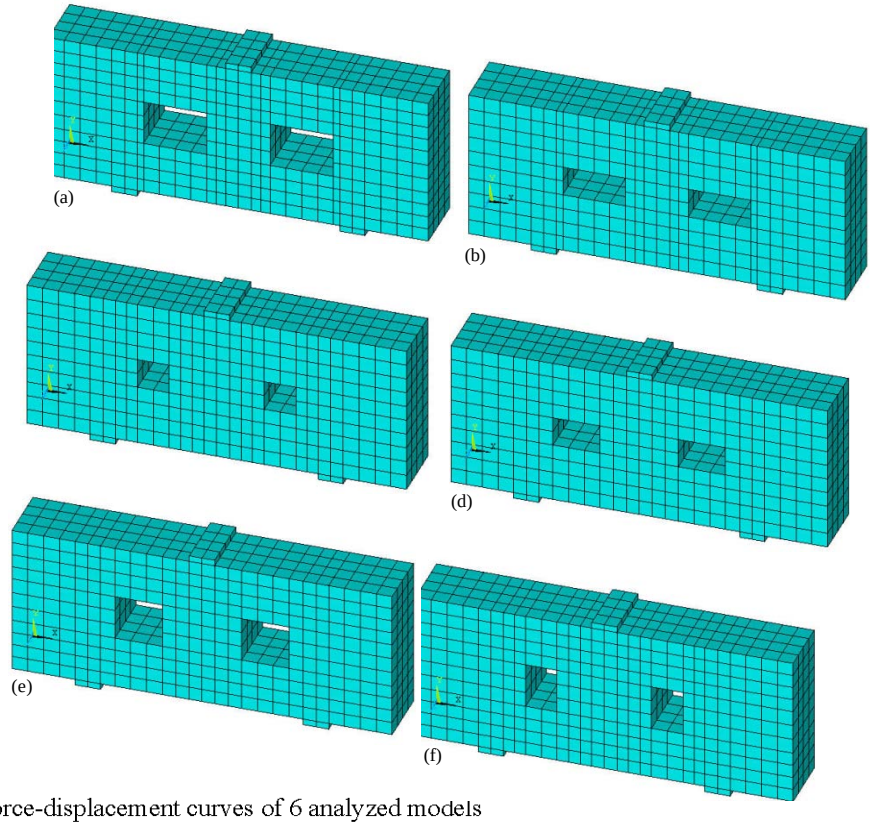

Fig. 14 (a-f): Force-displacement curves of 6 analyzed models

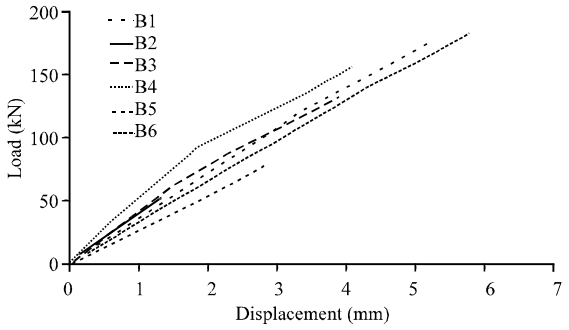

Fig. 15: Changes of area under force-displacement curve against angle

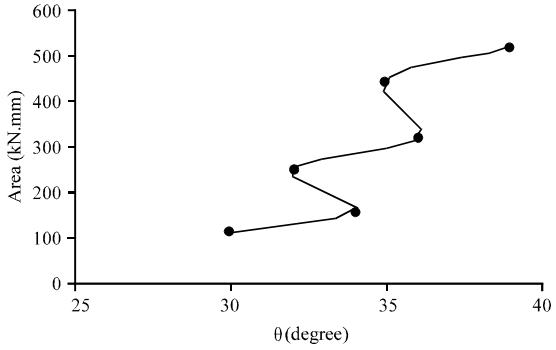

Fig. 16: Changes of concentrated load on beam center against Z2/L1

This curve consists of three zones each representing one group. L1 is the horizontal distance between two ends of the opening. In each group the loading capacity of beam increases by the decreases in parameter. In the first group a 33% decrease in parameter leads to a 28% increase in loading capacity of the beam. For a 33% decrease of in second and third groups the ultimate load increases 19 and 4%, respectively. In all groups by a 55% decrease in the final force of the beam increased by 126%.

6-2 cracking pattern. As shown in Fig. 17 by increasing opening's area in each group there was a decrease in the load which cracking occurred. In the all 6 models the maximum cracking displacement is 2.9 times of the minimum. The maximum displacement cracking is for B6 and the minimum happened at B1 specimen. The decrease rate of openings in first group is 33% and cracking displacement increases 19%. In second group by a 33% decrease of opening area the cracking displacement increases by 5%, this is 17% for the third group when it experienced the same decrease in opening area as the second group.The maximum opening area belongs to the first group and the least belongs to the third group.

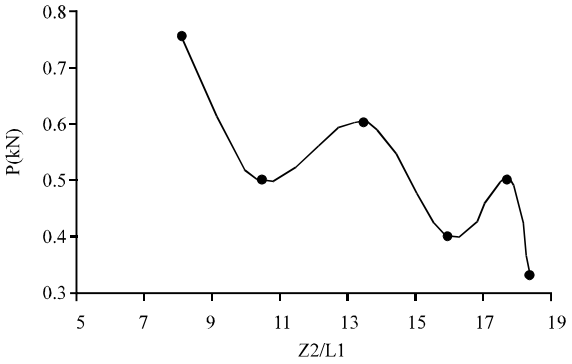

Fig. 17: Cracking changes based on opening's area percentage

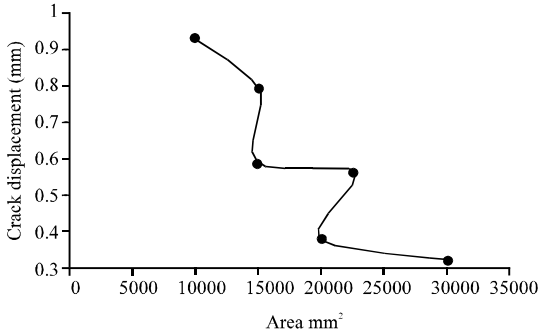

Fig. 18: Beam's ultimate changes of deflection curve against the total area of openings

Opening area of B6 decreases 67%, compared to B1. The medium cracking displacement for the first group is 0.351 mm and 0.575 for the second group and 0.86 for the third group.

In Fig. 18, beam's ultimate changes of deflection curve is shown against the total area of openings. Based on Fig. 19, B6 has the most displacement and B1 has the least displacement = 2.91 mm. the maximum amount for final displacement in the third group and specimen B6 is 5.81 mm which is 2 times of its minimum. By increase in opening dimensions the final displacement has decreased. In the first group by a 33% decrease in opening area, the ultimate displacement increases 8%. In second and third groups there is a 6 and 11% increase in ultimate displacement with the same increase in opening area as one of the first group. The rate of increase for the third group is more than the other two groups while the decrease rate of opening area is the same for all groups. The rate of opening area decrease in specimen B1-B6 compared to the first model is 67%. Despite that the ultimate displacement gets two fold.

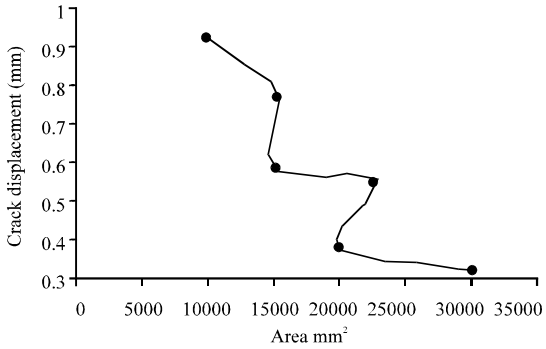

Fig. 19: Beam's ultimate changes of deflection curve against the total area of openings

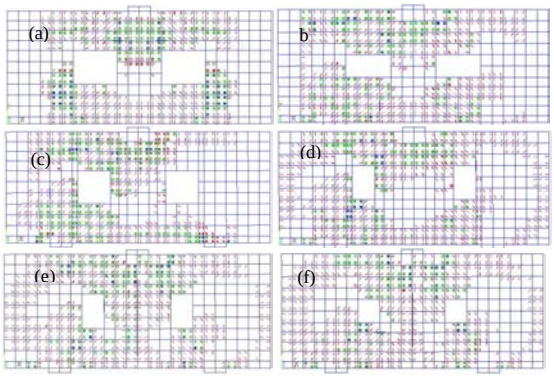

Fig. 20: Crack pattern of FEM models at ultimate load: a) B1; b) B2; c) B3; d) B4; e) B5 and f) B6

The cracking pattern of beams at ultimate load is depicted in Fig. 19 in which the plastic cracks in opening corners that are located on strut of compression truss could be observed. As it's shown in Fig. 20 a few flexural cracks at mid-span and at maximum moment points are emerged. The distribution of plastic cracks around opening corners is observed in a manner that they are more dense at opposing corners which align with compression element of the beam. On the zones between two openings considerable strains is observed.

Comparing finite element model and theoretical relations: There has been a comparison between results of finite element analysis of six concrete beams and those of theoretical relations. The results are summarized in Table 5. According to Table 5, it could be deduced that the maximum difference between theoretical results and finite element analysis results is 12.31%, the minimum amount between them is 6.52%. The average difference between finite element and theoretical results for first, second and third group is 7.4, 8.9 and10.8%, respectively.

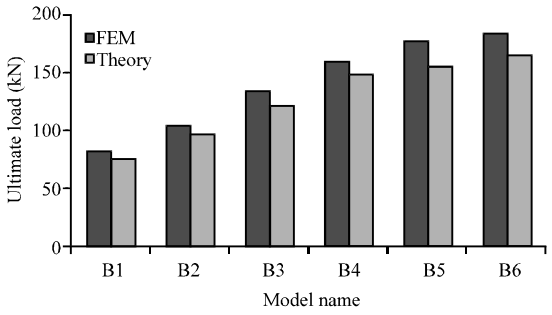

Fig. 21: Diagram of differences between results of FEM and theoretical models

In Fig. 21, one column depicts results from finite element results and the other results from theoretical model.

CONCLUSION

In this study the crack pattern in concrete deep beams is investigated. Based on the results from finite element models the following is concluded: By increase in dimensions of opening the stiffness of deep concrete beam reduces. This reduction helps cracking in deep beam to happen at smaller displacements. The maximum amount of cracking displacement in specimens is 2.9 times of its minimum. The increase of cracking load and displacement of second specimen comparing to first specimen of each group is 19, 30% for the first group, 5 and 19% in the second group and 18 and 7% in the third group. Likewise, the ultimate load and displacement in the first group is 28 and 8%, second group 19 and 6% and third group 4 and 11%.

The specimen with the smallest opening had the most displacement and the specimen with the largest opening had the least displacement. The maximum displacement is 5.81 mm which is twice its minimum amount. The displacement reduced by the increase in opening dimensions. In first, second and third groups the final displacement of beam increased by 8, 6 and 11% respectively, once the opening dimensions reduced by 33%. Besides plastic cracks are located around opening corners which are aligned with compression member of the truss and few flexural corners were spotted at mid-span and maximum moment zones. The distribution of cracks was mostly around corners which were aligned with compression member of the truss. The specimen with the smallest opening and farthest location form beam center has the most loading capacity. The specimen with the largest opening and closest to beam center has the least load capacity. The maximum load capacity is 2.27 times of the minimum. The maximum difference between theoretical calculations and finite element analysis is 12.31%. The minimum difference of them is 6.52%.

REFERENCES

ACI, 2002. Building Code Requirements for Structural Concrete (ACI 318-02) and Commentary (ACI 318R-02). American Concrete Institute, Farmington Hills, MI. USA, ISBN-13: 978-0870310652.

Damian, K., M. Thomas, Y. Solomon, C. Kasidit and P. Tanarat, 2001. Finite element modeling of reinforced concrete structures strengthened with FRP laminates. Oregon Department of Transportation, Salem, Oregon.

Gunel, M.H. and H.E. Ilgin, 2007. A proposal for the classification of structural systems of tall buildings. Build. Environ., 42: 2667-2675.

Islam, M.R., M.A. Mansur and M. Maalej, 2005. Shear strengthening of RC deep beams using externally bonded FRP systems. Cem. Concr. Compos., 27: 413-420.

Kong, F.K. and G.R. Sharp, 1977. Structural idealization for deep beams with web openings. Mag. Concr. Res., 29: 81-91.

Leong, C.L. and K.H. Tan, 2003. Proposed revision on CIRIA design equation for normal and high strength concrete deep beams. Mag. Concr. Res., 55: 267-278.

Lu, W.Y., 2006. Shear strength prediction for steel reinforced concrete deep beams. J. Constr. Steel Res., 62: 933-942.

Tan, K.H., F.K. Kong, S. Teng and L.W. Weng, 1997. Effect of web reinforcement on high-strength concrete deep beams. ACI. Struct. J., 94: 572-582.

Tan, K.H., K. Tong and C.Y. Tang, 2003. Consistent strut-and-tie modelling of deep beams with web openings. Mag. Concr. Res., 55: 65-75.

Zhang, N. and K.H. Tan, 2007. Direct strut-and-tie model for single span and continuous deep beams. Eng. Struct., 29: 2987-3001.